ARMY RESEARCH LABORATORY

Acoustic Nondestructive Evaluation of Aircraft Paneling Using Piezoelectric Sensors

by Eddie Elburn and Ryan C. Toonen

ARL-MR-834 **December 2012**

Approved for public release; distribution is unlimited.

NOTICES

Disclaimers

The findings in this report are not to be construed as an official Department of the Army position unless so designated by other authorized documents.

Citation of manufacturer's or trade names does not constitute an official endorsement or approval of the use thereof.

Destroy this report when it is no longer needed. Do not return it to the originator.

Army Research Laboratory
Aberdeen Proving Ground, MD 21005-5069

ARL-MR-834 **December 2012**

Acoustic Nondestructive Evaluation of Aircraft Paneling Using Piezoelectric Sensors

Eddie Elburn and Ryan C. Toonen
Weapons and Materials Research Directorate, ARL

Approved for public release; distribution is unlimited.

REPORT DOCUMENTATION PAGE	Form Approved OMB No. 0704-0188

Public reporting burden for this collection of information is estimated to average 1 hour per response, including the time for reviewing instructions, searching existing data sources, gathering and maintaining the data needed, and completing and reviewing the collection information. Send comments regarding this burden estimate or any other aspect of this collection of information, including suggestions for reducing the burden, to Department of Defense, Washington Headquarters Services, Directorate for Information Operations and Reports (0704-0188), 1215 Jefferson Davis Highway, Suite 1204, Arlington, VA 22202-4302. Respondents should be aware that notwithstanding any other provision of law, no person shall be subject to any penalty for failing to comply with a collection of information if it does not display a currently valid OMB control number.
PLEASE DO NOT RETURN YOUR FORM TO THE ABOVE ADDRESS.

1. REPORT DATE *(DD-MM-YYYY)*	2. REPORT TYPE	3. DATES COVERED (From - To)
December 2012	Final	August 2011

4. TITLE AND SUBTITLE
Acoustic Nondestructive Evaluation of Aircraft Paneling Using Piezoelectric Sensors

5a. CONTRACT NUMBER

5b. GRANT NUMBER

5c. PROGRAM ELEMENT NUMBER

6. AUTHOR(S)
Eddie Elburn and Ryan C. Toonen

5d. PROJECT NUMBER

5e. TASK NUMBER

5f. WORK UNIT NUMBER

7. PERFORMING ORGANIZATION NAME(S) AND ADDRESS(ES)
U.S. Army Research Laboratory
ATTN: RDRL-WMM-E
Aberdeen Proving Ground, MD 21005-5069

8. PERFORMING ORGANIZATION REPORT NUMBER
ARL-MR-834

9. SPONSORING/MONITORING AGENCY NAME(S) AND ADDRESS(ES)

10. SPONSOR/MONITOR'S ACRONYM(S)

11. SPONSOR/MONITOR'S REPORT NUMBER(S)

12. DISTRIBUTION/AVAILABILITY STATEMENT
Approved for public release; distribution is unlimited.

13. SUPPLEMENTARY NOTES

14. ABSTRACT
The U.S. Army Research Laboratory has constructed a nondestructive evaluation (NDE) system for monitoring structural health in aircraft paneling. Our system relies on commercially available Piezoelectric Wafer Active Sensors (PWASs). These sensors were bonded to 0.063-in-thick aircraft-grade high-strength aluminum (alloy 2024) sheets using commercially available strain gauge adhesive, and 22 arbitrary waveform generator hook-up wire was soldered to each one to establish electrical contact. Audio and ultrasonic burst-modulated sinusoidal signals were applied to a single PWAS using an arbitrary waveform generator. The acoustic response was detected by the remaining sensors and measured using an oscilloscope. The location of defects in the aircraft paneling was determined using a multilateration algorithm based on a cross-correlation technique. In order to test the detection limits of our NDE system, holes with a variety of diameters were intentionally drilled through the aluminum panels. Our system was able to detect holes with diameter sizes that were comparable to the panel thickness.

15. SUBJECT TERMS
PZT, PWAS, cross correlation, multilateration, oscilloscope, nondestructive evaluation

16. SECURITY CLASSIFICATION OF:			17. LIMITATION OF ABSTRACT	18. NUMBER OF PAGES	19a. NAME OF RESPONSIBLE PERSON
a. REPORT	b. ABSTRACT	c. THIS PAGE			19b. TELEPHONE NUMBER (*Include area code*)
Unclassified	Unclassified	Unclassified	UU	20	Eddie Elburn 410-306-4536

Standard Form 298 (Rev. 8/98)
Prescribed by ANSI Std. Z39.18

Contents

List of Figures

Acknowledgments

The authors thank the Integrated Electromagnetic Materials Team of the U.S. Army Research Laboratory, Weapons and Materials Research Directorate, Clinical Trials Monitoring Branch, for supporting this project. We would also like to thank the Science and Engineering Apprenticeship Program (SEAP) and George Washington University for giving Eddie Elburn the opportunity to participate in this internship, as well funding for the project. One final thanks goes out to Dr. Sandra Young for organizing the entire SEAP program.

INTENTIONALLY LEFT BLANK.

1. Introduction

Piezoelectric Wafer Active Sensors (PWASs) have multiple applications that would benefit the general population. Aircraft paneling is the major application for this project. Currently, military aircraft vehicles are retired after a specific age determined by cumulative usage. In some cases, these expiration dates are only one-fourth of the designed lifetimes. Case studies have shown that by implementing health-monitoring techniques, the service lives of legacy fleets could be extended to 250% of their designed life (*1*, *2*). With our system in place, sensors would search for defects in real time and alert an operator when the structural integrity of the vehicle has been compromised. In addition to extending the overall service lifetime, this technique would allow vehicles to fly for longer periods before requiring routine inspection. Potentially, this innovation could save the Department of Defense hundreds of millions of dollars per year (*1*, *2*).

Historically, methods for detecting defects in structures have included visual inspection, x-ray analysis, and ultrasonic acoustography. Visual inspection requires a technician to tediously scan an object while searching for defects or signs of compromised structural integrity. The inconvenience associated with this technique is that for every 1 h of use, the object is required to receive 10 human hours of inspection. Apart from consuming significant amounts of military personnel time, this requirement effectively reduces the number of vehicles available for executing operations, thereby weakening the strength of a fleet.

X-ray analysis uses x-ray shadowing to pinpoint the locations of defects in structures. The downfall of this technique is the requirement of bulky diaganostic equipment that is not readily field-deployable. Additionally, inspected parts must be removed from the aircraft in order to be placed in the x-ray machine. Disassembling and reassembling a system could introduce unforeseen mechanical problems.

Ultrasonic acoustography (*3*) determines if a defect is present by completing the following steps. First, the part to be inspected must be removed from the rest of the aircraft. Next, the part is submerged in a water tank. Afterwards, the part is rastered by a sensor, which identifies if a defect is present. The difficulties with this system are that it takes an hour to complete a somewhat small part, the part in question must be removed from the rest of the object, and a water submersion tank is required. Snapshot ultrasonic acoustography, considered an improvement over traditional acoustography, consists of a similar process except for taking a picture of the part instead of rastering. Snapshot reduces the amount of time to 3 min, but it still requires the water submersion tank.

To implement the PWASs in a nondestructive evaluation application, these sensors are bonded to the medium one wishes to monitor. Figure 1 shows a photograph of a PWAS being bonded to a strip of aircraft-grade aluminum. One of the PWASs is connected to an arbitrary waveform

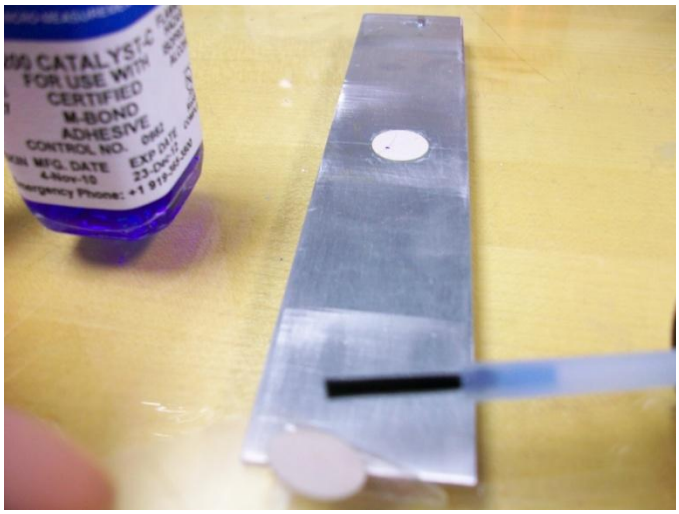

Figure 1. M-bond catalyst is applied to a PWAS for bonding procedure.

generator (AWG), which transmits pulses for the remaining sensors to receive. This information is then digitized by an oscilloscope and sent to a data acquisition laptop for signal processing. The signal-processing algorithm uses a cross-correlation technique to find the time of arrival (ToA) of a defect-scattered signal at each PWAS detection node. The coordinate of the defect is located by employing multilateration with the ToA information and the known coordinates of each sensor.

2. Procedure

The first procedure is bonding the commercial-off-the-shelf PWAS (10-mm diameter, 0.2 mm thick) (*4*) to an aircraft-grade high-strength aluminum (alloy 2024) 0.063-in-thick × 12- × 12-in plate. In order to bond the sensors to the aluminum, we used strain gauge adhesive (Vishay Precision Group M-Bond 200) (*5*). Once we bonded the sensors to the aluminum, they were soldered to 134-AWP solid copper wires (Vishay PG P/N F006484) and/or 22-AWG PVC-cladded stranded hook-up wires (Belden 8524). This completed the bonding and soldering process. The sensors held to the aluminum for roughly 1 week before the adhesive started to wear off, yet some sets stayed connected for over a month. With a more in-depth research of the topic, the bonding could have lasted for a longer period.

The next procedure was setting up the sensor arrangement and the rest of the system. We set up an arrangement featuring four PWASs. A four-sensor arrangement was chosen because it conserves sensors yet still covers the entire plate. The more sensors we included, the better chance we would have of detecting a defect.

One of the sensors was attached to an Agilent 33220A AWG. This AWG sends burst-modulated sinusoidal signals through the first PWAS, through the aluminum medium, and then finally through the other three receiving PWASs. We experimented with signal frequencies ranging from 10 Hz to 20 MHz; however, we ultimately decided to employ 350 kHz as the frequency of our carrier wave because previous research indicated that this frequency yields a maximal response in an aluminum medium (*4*). Using a higher frequency yields increased defect detection resolution. For this reason, we plan on employing novel thin film sensors that operate at higher ultrasonic frequencies in subsequent studies.

In figure 2, the PWAS in the upper left-hand corner is the acting transducer connected to the AWG. The other three PWASs are being used as receiving sensors, which send the information they detect to an Agilent DSO1024A oscilloscope. Near the top-right corner of figure 2 is a yellow aligator clip attached to the side of the aluminum plate. The ground of each sensor is also connected to this clip. This electrical connection ensures single-point grounding, which has been implemented to avoid electromagnetic interference that could be induced in a ground loop.

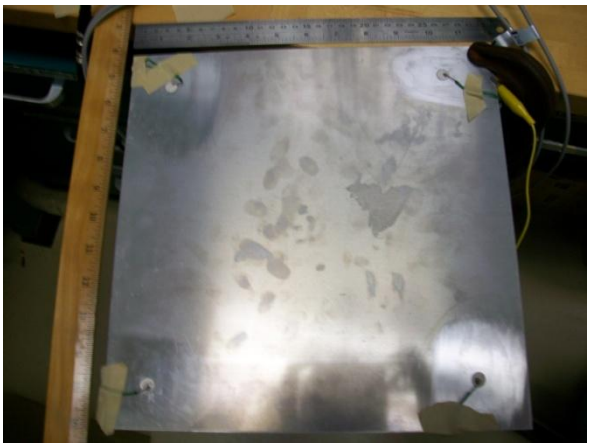

Figure 2. Four PWASs arranged on a high-strength aluminum plate.

3. Retrieving Data

Figure 3 displays four waveforms. The top waveform is the input sensor (the one connected to the AWG). The other three signals were received from the detector nodes. At the very beginning of each waveform (on the left side of the graph), the signals are similar in appearance. The received (bottom three) waveform of each sensor features an electromagnetic pick-up signature that is aligned with the transduced signal but phase shifted by 180°. We know to disregard these nonacoustic waveforms, as they occur almost instantaneously—the information traveled near the speed of light rather than the speed of sound. The bumps and curves found

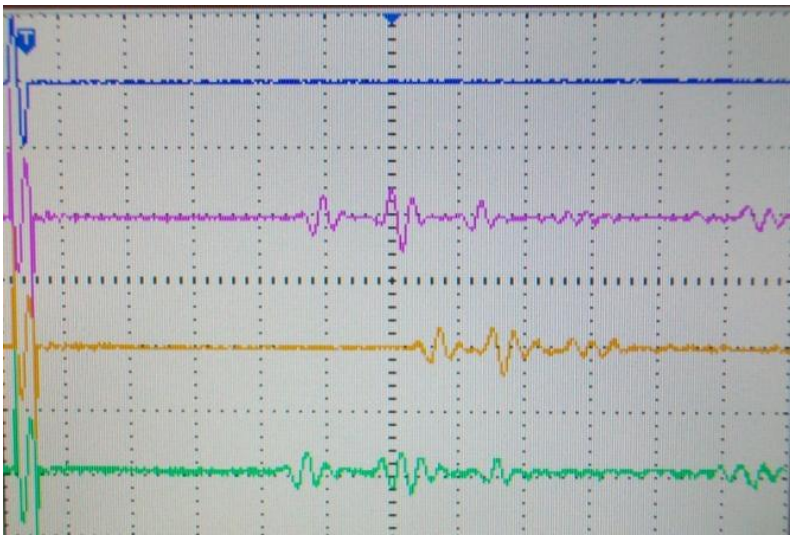

Figure 3. Graph showing all four PWAS waveforms as amplitude is a function of time.

after the initial mark are generated by the acoustic signals and their echoes. These electrical signatures generated by the scattered ultrasonic waves reveal data that can be used to pinpoint the location of a defect. As expected, the three waveforms have different relative time delays corresponding to their distances from the transmitter.

To process the received waveforms, we created a Labview program. Our program acquires its data directly from the oscilloscope. Figure 4 shows the graphical user interface of our program. A user may specify measurement conditions in addition to viewing the graphical representations of the acquired data and Cartesian location of a defect. The four rectangular graphs in a column represent the four waveforms. This ordering is the same as that of the graphical representation on the oscilloscope, which is essential for artifacts arising from inappropriate scaling of the voltage axes.

We used cross correlation to accurately calculate the time delay between sending and receiving signals with similar profiles. Using the cross-correlation equation (eq. 1), we can merge two waveforms.

$$V_S \otimes V_M[n] \equiv \sum_{m=0}^{M-1} V_S^*[m] \cdot V_M[n+m]. \qquad (1)$$

Equation 1 describes the cross-correlation algorithm (*6*). The variable n is the index of discrete time, M is the total number of data points collected from the oscilloscope, and V_S and V_M are the sourced and measured voltage waveforms, respectively. With this formula, we individually cross correlate the transmitted waveform (waveform 1) against each of the detected waveforms (waveforms 2, 3, and 4). Local maxima in the cross-correlation waveform indicate ToAs from defects (points of acoustic scattering).

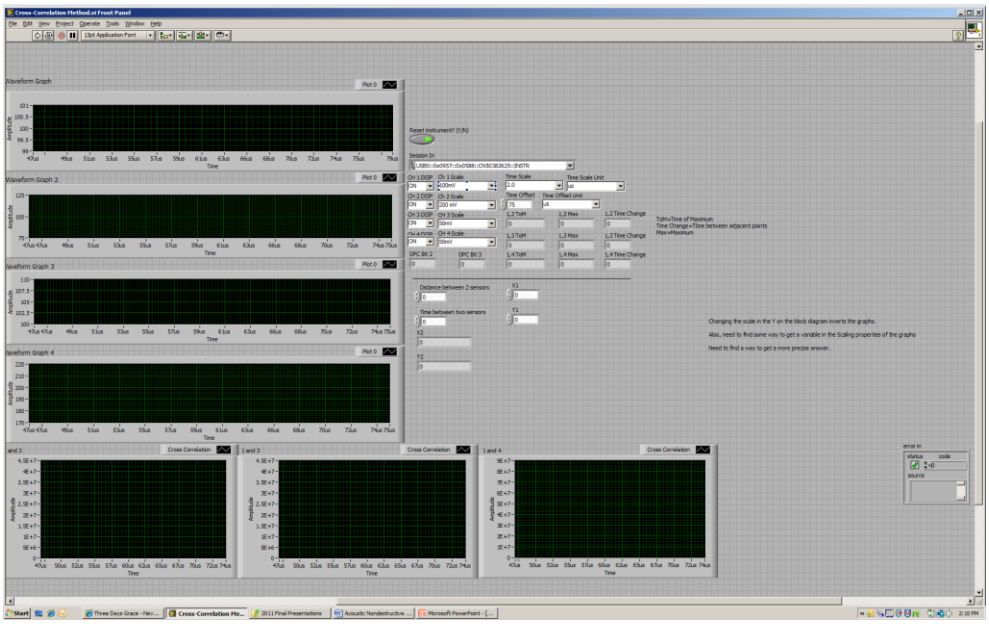

Figure 4. Front panel of the program used to determine defect location.

In figure 5, the cross-correlation algorithm has been applied to the data received from a bare sheet of aluminum—no defects were intentionally introduced. The cross-correlation products denoted as series 1, 2, and 3 correspond to the correlation between waveforms 1 and 2, 1 and 3, and 1 and 4, respectfully. It is evident that there are peaks present in these graphs. Ideally, one might assume that data collected from an aluminum plate with no introduced defects would yield no nonzero peaks in the cross-correlation waveform. However, because of the finite expanse of the panel, signals echo off of the perimeter. For this reason, it is necessary to compare any diagnostic cross-correlation waveform with that acquired when the structure contained such significant defects.

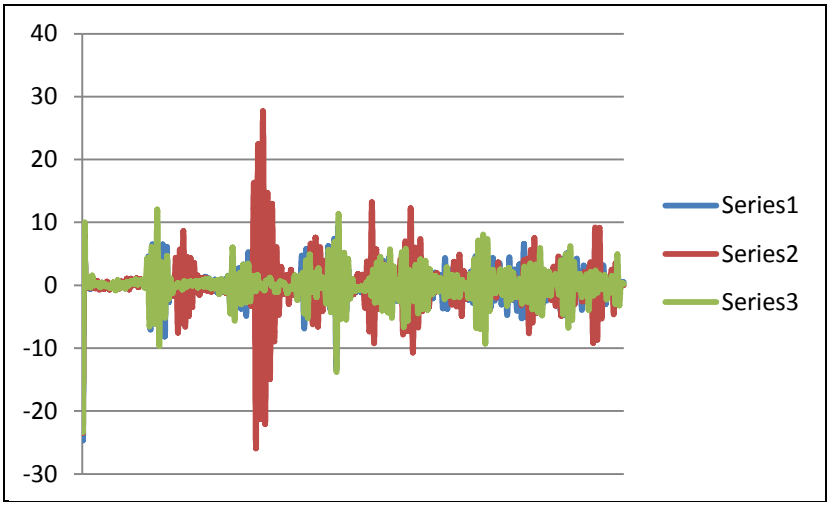

Figure 5. The cross-correlation algorithm being applied to the sheet of aluminum containing no defects.

4. Defects

To demonstrate our system's capability of defect detection, defects were placed in an aluminum sheet. The intentionally introduced defects were realized by drilling holes in the sheet with a drill press. Initially, a 1/8-in-diameter hole was drilled near the center of the sheet. The diameter was chosen to be roughly twice the thickness of the 0.063-in-thick sheet. Following this step, a defect detection experiment was performed and the data was saved. Next, a second 1/8-in-diameter hole was drilled an inch away. Data was collected following this step to determine if two closely spaced holes could be individually resolved using our detection process. Then, a third hole with a diameter approximately equal to the sheet thickness was drilled in a location opposite the first hole with respect to the center of the sheet. The data shown in figure 6 represents cross-correlation data collected from the aluminum sheet with the three intentionally introduced artificial defects (the three holes).

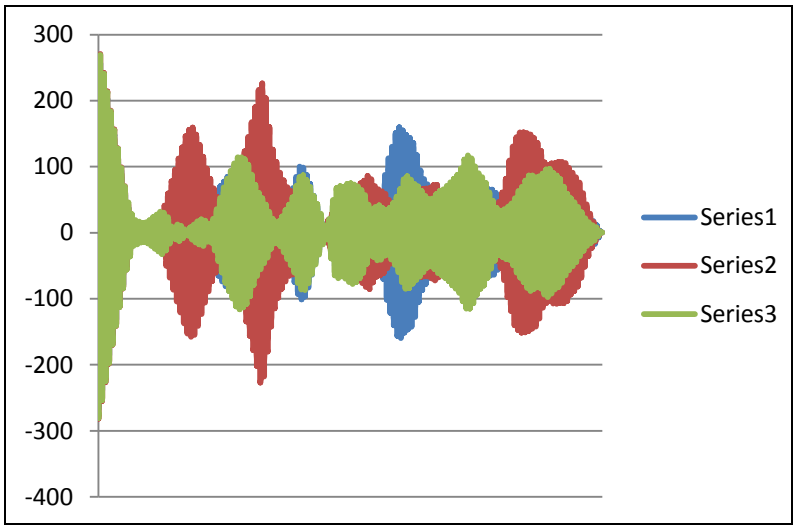

Figure 6. The cross-correlation algorithm being applied to the sheet of aluminum containing three separate defects.

When figure 6 is compared to figure 5, differences are clearly present. This means that adding defects to the aluminum sheet increased the amplitude of the graphs, which corresponds to an increase in the time delay between sensors. Once we had distinguished that differences were present between the graphs, we decided to initiate one more defect in the sheet. The final defect was a quarter-inch defect, or four times the thickness of the sheet. The main goal of this experiment was to determine what sections of the graph changed the most when a defect was present. Figure 7 shows data for the aluminum sheet containing four defects, including the large defect.

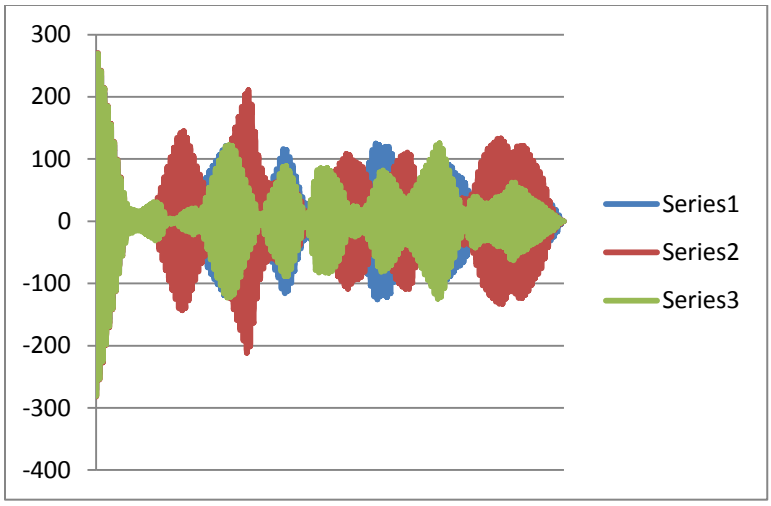

Figure 7. The cross-correlation algorithm being applied to the sheet of aluminum containing four separate defects.

Comparing the two graphs, it is evident that while the differences are not substantial, they are present. The green graph as a whole seems to increase slightly, and the ending portion of the red graph is larger than before. Using this data, we can calculate the exact location of the defect. In future efforts, we will attempt to implement a decorrelation algorithm to remove the echoic signatures from nondefects that contribute to acoustic scattering. From a practical point of view, such a scheme will be necessary for subtracting out the effects of intentional irregularities, including bolts, rivets, and panel edges. Such a technique will involve characterizing the system in a state of good health to establish a baseline for future comparisons.

5. Algorithm

To calculate the exact location, we need to use an algorithm specially designed for this problem. This algorithm works specifically for a four-sensor arrangement in a square formation, but other algorithms can be used for different situations. The algorithm is based off of figure 8. Using information gathered by the oscilloscope, we can calculate the exact location of the defect.

The basics for the algorithm start with the basic velocity, distance, and time equation, and then implementing that into the Pythagorean theorem.

$$\begin{aligned} V_0 &= d/t \\ d &= V_0 \cdot t \\ a^2 + b^2 &= c^2 \end{aligned} \quad . \tag{2}$$

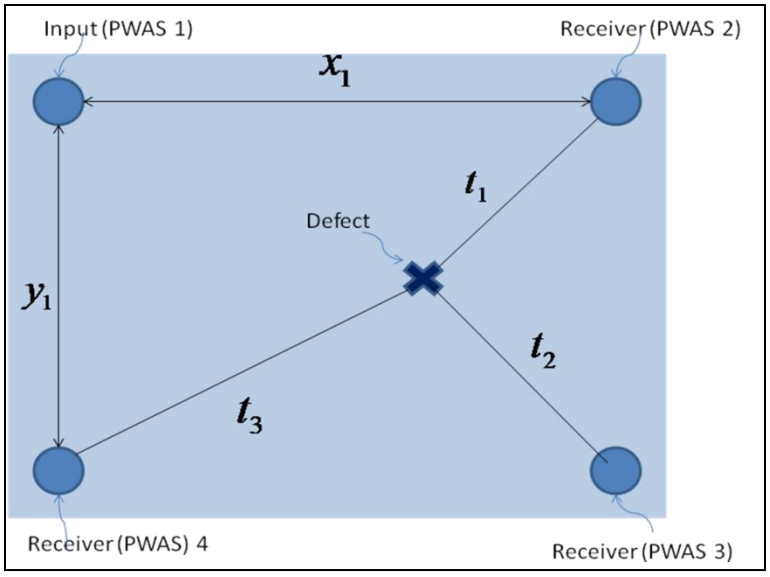

Figure 8. The diagram shows all four PWASs working in the system. Also pictured is the aluminum plate as well as a microscopic defect.

Once the velocity formula has been plugged into the Pythagorean theorem, simplification can be used to come up with the three starting equations of the algorithm.

$$\begin{aligned} d_1 &= V_0 \cdot t_1 = \sqrt{(x_2)^2 + (y_2 - y_1)^2} \\ d_2 &= V_0 \cdot t_2 = \sqrt{(x_2 - x_1)^2 + (y_2 - y_1)^2} \\ d_3 &= V_0 \cdot t_3 = \sqrt{(x_2 - x_1)^2 + (y_2)^2} \end{aligned} \quad . \qquad (3)$$

d is equal to the distance between the sensor and the defect. This should not be misunderstood for x_2, y_2, which shows the actual location. This variable is substituted out in the latter part of the simplifying.

V_0 is equal to the velocity, which the signal passes through the medium. This can be referenced from previously published work, or it can be calculated by finding the distance between two sensors and dividing that number by the time it takes for the signal to go that distance, which can be found using the oscilloscope.

t is equal to the time delay between the sensor and the defect. This value is found from the cross-correlation algorithm mentioned earlier.

x_1, y_1 are equal to the length and width of the medium used, where x_1 corresponds to sensor 2, or time delay 1, and y_1 corresponds to sensor 4, or time delay 3.

x_2, y_2 are equal to the pinpointed location of the defect. Once the other information has been plugged into the equations, the final information of interest can be calculated.

After squaring all three main equations, we use the elimination method for simplifying systems of equations to find two equations to solve for the variables required.

$$\begin{aligned} d_2^{\,2} - d_1^{\,2} &= (x_2 - x_1)^2 - (x_2)^2 \\ d_2^{\,2} - d_3^{\,2} &= (y_2 - y_1)^2 - (y_2)^2 \end{aligned}. \tag{4}$$

After multiple steps of simplification, the equations now look like this:

$$x_2 = \frac{x_1^{\,2} + d_1^{\,2} - d2^2}{2x_1}, y_2 = \frac{y_1^{\,2} + d_3^{\,2} - d2^2}{2y_1}. \tag{5}$$

Next, we need to plug back V_0 and t to get a general equation for x_2 and y_2. Once this has been completed, we use the distributive postulate to simplify the equation to the final two net equations.

$$x_2 = \frac{x_1}{2} + \frac{V_0^{\,2}(t_1^{\,2} - t_2^{\,2})}{2x_1}, y_2 = \frac{y_1}{2} + \frac{V_0^{\,2}(t_3^{\,2} - t_2^{\,2})}{2y_1}. \tag{6}$$

6. Conclusion

In conclusion, a system of sensors has been developed that can detect defects in the structures of metals. There are numerous applications for this system involving safety of vehicles and structures. In addition to reducing the number of Soldier fatalities, this real-time monitoring system could potentially prevent the unnecessary deaths of citizens due to structural failure. A simple algorithm was constructed to accurately pinpoint the location of the defect, thus making the system more time efficient than other defect detector systems. Current efforts are underway to employ an improved algorithm that can subtract out the acoustic signatures of nondefect irregularities.

We constructed a relatively simple apparatus. Future improvements, including the addition of ultrasonic thin film piezoelectric sensors, could be used to improve the functionality of the system. By using such sensors in place of the PWASs, we can implement acoustic test signals of higher frequencies (approaching tens or even hundreds of megahertz). Using a higher-frequency test signal will increase the defect detection resolution. Additionally, miniaturized antennas may also be implemented to eliminate the need for wires in our system. Such an advancement will make placement of the sensor nodes more time efficient and cost effective. While this system provides an improved method for locating structural defects, there are still additional hardware and software developments that could be made to enhance its performance.

7. References

1. White, D. J.; Vaughan, R. E. Fleet Usage Monitoring Is Essential in Improving Aging U.S. Army Helicopter Safety, Availability, and Affordability. *Proceedings of the 9th Joint FAA/DOD/NASA Conference on Aging Aircraft*, JCAA, Atlanta, GA, 2006.
2. Ernst, R. P. Aging Aircraft National Strategy. *Proceedings of the 6th Annual System Engineering Conference*, NDIA, San Diego, CA, 2003.
3. Santec Systems, Inc., Web site. Acoustography. http://www.santecsystems.com/acoustography.htm (accessed 15 August 2011).
4. Giurgiutiu, V.; Zagrai, A. N.; Bao, J. J. *Structural Health Monitoring* **2002**, *1*, 41–61.
5. Vishay PG Instruction Bulletin B-127-14; Document No.:11127, Revision 14-Oct-11; Malvern, PA, 2011.
6. J. P. Lewis Web site. Lewis, J. P. Fast Normalized Cross-Correlation. http://scribblethink.org/Work/nvisionInterface/nip.html (accessed 17 August 2011).

NO. OF COPIES	ORGANIZATION
1 (PDF only)	DEFENSE TECHNICAL INFORMATION CTR DTIC OCA 8725 JOHN J KINGMAN RD STE 0944 FORT BELVOIR VA 22060-6218
1	DIRECTOR US ARMY RESEARCH LAB IMAL HRA 2800 POWDER MILL RD ADELPHI MD 20783-1197
1	DIRECTOR US ARMY RESEARCH LAB RDRL CIO LL 2800 POWDER MILL RD ADELPHI MD 20783-1197

NO. OF
COPIES ORGANIZATION

ABERDEEN PROVING GROUND

3 DIR USARL
RDRL WM
S YOUNG
RDRL WMM E
R TOONEN (2 CPS)